

6. Lastly, we shall discuss the weak interaction of leptons. If we assume that the neutrino belongs to the singlet state in the M space, we have good reason to expect exclusively the $V-A$ interaction for the decay process involving the emission of neutrinos, since then the interaction terms which are S pseudo-invariant and

X pseudo-invariant will be lost. We could thus extend the principle of SX invariance to the universal $V-A$ theory^{9,20,21} for the weak interaction of leptons.

²⁰ R. P. Feynman and M. Gell-Mann, Phys. Rev. **109**, 193 (1958).

²¹ R. H. Dalitz, Revs. Modern Phys. **31**, 823 (1959).

PHYSICAL REVIEW

VOLUME 122, NUMBER 5

JUNE 1, 1961

Direct Nucleon-Nucleon Collisions inside the Nucleus According to the Impulse Approximation*

LESTER WINSBERG AND THOMAS P. CLEMENTS

Lawrence Radiation Laboratory, University of California, Berkeley, California

(Received November 18, 1960)

Direct nucleon-nucleon collisions play an important role in high-energy nuclear reactions. The importance of such collisions at lower energies is not clear. To aid in the interpretation of nuclear reactions, we have analyzed the collisions between an incident nucleon and nucleons in a Fermi gas by means of the impulse approximation. The treatment given here is based on information from nucleon-nucleon scattering experiments. Collisions inside a nucleus are considered to be the same as those in the unbound state at the same center-of-mass energy, except for the effect of the Pauli exclusion principle. The effective elastic

and inelastic cross section, $\langle\sigma\rangle$, between like and unlike nucleons is computed for incident energies from 10 Mev to 6 Bev at several values of the Fermi energy. The properties of the struck nucleons in allowed collisions are also calculated. This information may prove useful in interpreting some recoil experiments. Analytical expressions for $\langle\sigma\rangle$ and quantities related to the struck nucleon are given for elastic collisions in which the scattering is isotropic and the free-particle cross sections are either constant or vary inversely as the bombarding energy.

THE processes that occur during a nuclear reaction are not well known. One usually assumes that the collision between a high-energy particle and a nucleon inside a nucleus is essentially the same as in the unbound state at the same center-of-mass energy, except for the effect of the Pauli exclusion principle. In line with this "impulse approximation," information obtained from p - p , n - p , and π - p scattering experiments has been used in the analysis of nuclear reactions induced by high-energy particles.¹ This type of analysis has been successful in interpreting the available information on reactions induced by particles with energies of 1 Bev or less. However, serious discrepancies appear at higher energies.²

An analysis of nuclear reactions by means of the impulse approximation would be facilitated if the values of the effective collision cross sections $\langle\sigma\rangle$ of neutrons and protons inside nuclear matter were known at all energies. This information would be especially helpful for a study of the simpler reactions in which one or at most a few nucleons are emitted. The distance the incident particle penetrates the nucleus and the probability of escape of the collision products could be directly calculated from the values of $\langle\sigma\rangle$. The experimentally determined values of the cross sections, angu-

lar distributions, and kinetic energies of the products of the simpler nuclear reactions could then be compared with the results of a "one-step" calculation. In the calculation of Metropolis *et al.*, these reactions are treated along with all the other reactions that occur.¹

The values of $\langle\sigma\rangle$ have been previously estimated over a restricted range of incident energies, usually limited to cases in which the scattering is isotropic in the center-of-mass system.³⁻⁹ Because of their usefulness, we present analytical expressions for $\langle\sigma\rangle$ and for various quantities related to the momentum of the struck nucleons in allowed collisions. Here we consider only isotropic elastic scattering in which the free-particle cross section remains constant or varies inversely with energy.

The analytical solution of the general case is very complex. For this reason we have computed $\langle\sigma\rangle$ and the properties of the struck nucleons, by means of the Monte Carlo method, for incident energies from 10 Mev to 6 Bev at several values of the Fermi energy.¹⁰

³ M. L. Goldberger, Phys. Rev. **74**, 1269 (1948).

⁴ Y. Yamaguchi, Progr. Theoret. Phys. (Kyoto) **5**, 332 (1950).

⁵ S. Hayakawa, M. Kawai, and K. Kikuchi, Progr. Theoret. Phys. (Kyoto) **13**, 415 (1955).

⁶ E. Clemental and C. Villi, Nuovo cimento **2**, 176 (1955).

⁷ I. G. Ivanter and L. B. Okun, Zhur. Eksptl. i Teoret. Fiz. **32**, 402 (1957) [English translation: Soviet Phys.—JETP **5**, 340 (1957)].

⁸ R. M. Sternheimer, Phys. Rev. **106**, 1027 (1957).

⁹ J. R. Fulco, Phys. Rev. **114**, 374 (1959).

¹⁰ T. P. Clements and L. Winsberg, University of California Radiation Lab. Rept. UCRL-8982 (1960) (unpublished). This report contains a more complete description of the results than can be presented here.

*Based on work performed under the auspices of the U. S. Atomic Energy Commission.

¹ N. Metropolis, R. Bivins, M. Storm, A. Turkevich, J. M. Miller, and G. Friedlander, Phys. Rev. **110**, 185, 204 (1958). Further references are given there.

² D. R. Nethaway and L. Winsberg, Phys. Rev. **119**, 1375 (1960). Further references are given there.

TABLE I. Nonrelativistic expressions of $\langle\sigma\rangle$ and other quantities for isotropic scattering, where $\sigma=\sigma_0$ and $E_1 \geq 2E_F$.

(a)	$\langle\sigma\rangle = \sigma_0 \left(1 - \frac{7}{5}F\right)$
(b)	$\langle p_2 \rangle = 3p_F\sigma_0 \left(1 - \frac{4}{3}F\right) / 4\langle\sigma\rangle$
(c)	$\langle \cos\omega \rangle = -p_F\sigma_0 \left(1 - \frac{4}{3}F\right) / 4p_1\langle\sigma\rangle = -\langle p_2 \rangle / 3p_1$
(d)	$\langle p_2 \cos\omega \rangle_{\cos\omega > 0} = 3p_F\sigma_0 \left(1 - \frac{8}{15}F^{\frac{1}{2}} - \frac{7}{6}F + \frac{24}{35}F^{\frac{3}{2}} - \frac{11}{48}F^2\right) / 16\langle\sigma\rangle$
(e)	$\langle p_2 \cos\omega \rangle_{\cos\omega < 0} = -3p_F\sigma_0 \left(1 + \frac{8}{15}F^{\frac{1}{2}} - \frac{7}{6}F - \frac{24}{35}F^{\frac{3}{2}} + \frac{11}{48}F^2\right) / 16\langle\sigma\rangle$
(f)	$\langle p_2 \sin\omega \rangle = 3\pi p_F\sigma_0 \left(1 - \frac{17}{12}F + \frac{37}{384}F^2\right) / 16\langle\sigma\rangle$

In our treatment the nucleus is assumed to consist of neutron and proton Fermi gases. Collisions between two protons and between two neutrons are considered to be equivalent.

Finally, we compare the values obtained from the analytical expressions with the computed values. The information about the struck nucleons may prove useful in interpreting some recoil experiments.

ANALYTICAL EXPRESSIONS FOR ISOTROPIC ELASTIC SCATTERING

In this section we present analytical solutions for $\langle\sigma\rangle$ and the quantities related to the momentum of the struck nucleons for elastic collisions in which the

scattering is isotropic in the center-of-mass system, and the free-particle cross section either remains constant or varies inversely with energy. The latter type of cross-section dependence occurs below 150 Mev for both p - p and n - p collisions. Above this energy the elastic p - p cross section is nearly constant until about 1 Bev.¹¹

For elastic collisions between particles of the same rest mass, m_0 , the final energy of each particle, is given by

$$E_{\text{final}} = \frac{E_1 + E_2}{2} \pm \frac{E_1 - E_2}{2} \cos\theta' \\ \pm \frac{p_1 p_2}{[2(A+1)]^{\frac{1}{2}}} \sin\omega \sin\theta' \cos\Phi', \quad (1)$$

TABLE II. Relativistic expressions of $\langle\sigma\rangle$ and other quantities for isotropic scattering, where $\sigma=\sigma_0$ and $E_1 \geq 2E_F$.

(a)	$\langle\sigma\rangle = \sigma_0 \left[1 - \frac{7}{5}F - \frac{\gamma_1^3 + \gamma_1^2 - 2}{5\gamma_1^2(\gamma_1 + 1)}F\right]$
(b)	$\langle p_2 \rangle = 3p_F\sigma_0 \left[1 - \frac{4}{3}F - \frac{2(\gamma_1^3 + \gamma_1^2 - 2)}{9\gamma_1^2(\gamma_1 + 1)}F\right] / 4\langle\sigma\rangle$
(c)	$\langle \cos\omega \rangle = -p_F\sigma_0 \left[1 - \frac{4}{3}F + \frac{2(4\gamma_1^5 - 3\gamma_1^4 - 3\gamma_1^3 - 4\gamma_1^2 + 6)}{15\gamma_1^2(\gamma_1 + 1)}F\right] / 4\gamma_1 p_1 \langle\sigma\rangle$
(d)	$\langle p_2 \cos\omega \rangle_{\cos\omega > 0} = 3p_F\sigma_0 \left\{1 - \frac{8}{15\gamma_1} \left(\frac{2}{\gamma_1 + 1}\right)^{\frac{1}{2}} F^{\frac{1}{2}} - \frac{1}{3} \left[4 + \frac{\gamma_1^2 - 2}{\gamma_1^2(\gamma_1 + 1)}F\right]\right\} / 16\langle\sigma\rangle$
(e)	$\langle p_2 \cos\omega \rangle_{\cos\omega < 0} = -3p_F\sigma_0 \left\{1 + \frac{8}{15\gamma_1} \left(\frac{2}{\gamma_1 + 1}\right)^{\frac{1}{2}} F^{\frac{1}{2}} - \frac{1}{3} \left[4 + \frac{\gamma_1^2 - 2}{\gamma_1^2(\gamma_1 + 1)}F\right]\right\} / 16\langle\sigma\rangle$
(f)	$\langle p_2 \sin\omega \rangle = 3\pi p_F\sigma_0 \left\{1 - \frac{1}{3} \left[4 + \frac{2\gamma_1^3 + \gamma_1^2 - 2}{2\gamma_1^2(\gamma_1 + 1)}F\right]\right\} / 16\langle\sigma\rangle$

¹¹ W. N. Hess, Revs. Modern Phys. **30**, 368 (1958).

Table III. Nonrelativistic expressions of $\langle\sigma\rangle$ and other quantities for isotropic scattering, where σ is proportional to $1/E''$ and $E_1 \geq 2E_F$.

(a)	$\langle\sigma\rangle = \sigma_0 \left(1 - \frac{8}{5}F + \frac{16}{35}F^2 \right)$
(b)	$\langle p_2 \rangle = 3p_F \sigma_0 \left(1 - \frac{14}{9}F + \frac{23}{45}F^2 \right) / 4\langle\sigma\rangle$
(c)	$\langle \cos\omega \rangle = p_F \sigma_0 \left(1 - \frac{6}{5}F + \frac{1}{120}F^2 \right) / 4p_1 \langle\sigma\rangle$
(d)	$\langle p_2 \cos\omega \rangle_{\cos\omega > 0} = 3p_F \sigma_0 \left(1 + \frac{8}{15}F^{\frac{1}{2}} - \frac{7}{6}F - \frac{64}{105}F^{\frac{3}{2}} - \frac{5}{48}F^2 \right) / 16\langle\sigma\rangle$
(e)	$\langle p_2 \cos\omega \rangle_{\cos\omega < 0} = -3p_F \sigma_0 \left(1 - \frac{8}{15}F^{\frac{1}{2}} - \frac{7}{6}F + \frac{64}{105}F^{\frac{3}{2}} - \frac{5}{48}F^2 \right) / 16\langle\sigma\rangle$
(f)	$\langle p_2 \sin\omega \rangle = 3\pi p_F \sigma_0 \left(1 - \frac{7}{4}F + \frac{299}{384}F^2 \right) / 16\langle\sigma\rangle$

where E_1 and E_2 and p_1 and p_2 are the energies and momenta of the incident and struck particles, respectively, ω is the collision angle, and $A = \gamma_1 \gamma_2 - p_1 p_2 \cos\omega$. Quantities in the center-of-mass system are denoted by primed symbols: θ' is the scattering angle and Φ' is the azimuthal angle. The incident energy, E_1 , is defined here as the energy of the incident particle inside the nucleus, i.e., the sum of its energy outside the nucleus and the energy of the potential well. For our purposes it is unnecessary to specify either of the latter two quantities, merely their sum. In this paper velocities, denoted by β , are in units of c , the velocity of light; momenta, p , are given in units of $m_0 c$, and the kinetic energies, E , in units of $m_0 c^2$. The total energy of a particle in these units is $\gamma = 1 + E$. The $+$ sign of the

second and third terms in Eq. (1) is for the incident particle, and the $-$ sign is for the struck particle. A general equation for the elastic and inelastic cases is given in reference 10.

The effective nucleon-nucleon collision cross section inside nuclear matter is given by

$$\langle\sigma\rangle = \frac{1}{2} \int \int \int_{\beta_1}^{\beta''} -P(p_2) dp_2 d\cos\omega \frac{d\sigma}{d\Omega}(E'', \theta') d\Omega, \quad (2)$$

where β'' and E'' are the velocity and kinetic energy, respectively, of the incident particle in the coordinate system of the struck particle, $P(p_2) dp_2$ is the distribution in magnitude of the momenta of the struck particles, $d\sigma/d\Omega$ is the differential cross section, and E''

TABLE IV. Relativistic expressions of $\langle\sigma\rangle$ and other quantities for isotropic scattering, where σ is proportional to $1/E''$ and $E_1 \geq 2E_F$.

(a)	$\langle\sigma\rangle = \sigma_0 \left[1 - \frac{7}{5}F - \frac{\gamma_1^4 + \gamma_1^2 + 2\gamma_1 - 2}{5(\gamma_1 + 1)}F \right]$
(b)	$\langle p_2 \rangle = 3p_F \sigma_0 \left[1 - \frac{4}{3}F - \frac{\gamma_1^4 + \gamma_1^2 + 2\gamma_1 - 2}{9\gamma_1^2(\gamma_1 + 1)} \times 2F \right] / 4\langle\sigma\rangle$
(c)	$\langle \cos\omega \rangle = p_F \sigma_0 (\gamma_1^2 + \gamma_1 - 1) \left[1 - \frac{4}{3}F - \frac{4\gamma_1^6 + 5\gamma_1^5 - 8\gamma_1^4 + \gamma_1^3 - 4\gamma_1^2 - 6\gamma_1 + 6}{15(\gamma_1 + 1)(\gamma_1^2 + \gamma_1 - 1)} \times 2F \right] / 4\gamma_1 p_1 \langle\sigma\rangle$
(d)	$\langle p_2 \cos\omega \rangle_{\cos\omega > 0} = 3p_F \sigma_0 \left[1 + \frac{8}{15} \frac{\gamma_1^2 + \gamma_1 - 1}{\gamma_1} \left(\frac{2}{\gamma_1 + 1} \right)^{\frac{1}{2}} F^{\frac{1}{2}} - \frac{4}{3}F + \frac{2\gamma_1^3 - \gamma_1^2 - 2\gamma_1 + 2}{3\gamma_1^2(\gamma_1 + 1)}F \right] / 16\langle\sigma\rangle$
(e)	$\langle p_2 \cos\omega \rangle_{\cos\omega < 0} = -3p_F \sigma_0 \left[1 - \frac{8}{15} \frac{\gamma_1^2 + \gamma_1 - 1}{\gamma_1} \left(\frac{2}{\gamma_1 + 1} \right)^{\frac{1}{2}} F^{\frac{1}{2}} - \frac{4}{3}F + \frac{2\gamma_1^3 - \gamma_1^2 - 2\gamma_1 + 2}{3\gamma_1^2(\gamma_1 + 1)}F \right] / 16\langle\sigma\rangle$
(f)	$\langle p_2 \sin\omega \rangle = 3\pi p_F \sigma_0 \left[1 - \frac{4}{3}F - \frac{2\gamma_1^4 + 2\gamma_1^3 + \gamma_1^2 + 2\gamma_1 - 2}{6(\gamma_1 + 1)\gamma_1^2}F \right] / 16\langle\sigma\rangle$

equals $A-1$. The normalization factor $\frac{1}{2}$ arises from the integration with respect to $\cos\omega$ between $+1$ and -1 . The other limits of integration are set by the requirement that the energy of each product of the collision be greater than the Fermi energy, E_F . For this purpose we set E_{final} equal to E_F in Eq. (1) and in equivalent expressions for inelastic collisions.

The average value of any variable x in permitted collisions is

$$\langle x \rangle = \langle \sigma x \rangle / \langle \sigma \rangle, \quad (3)$$

where $\langle \sigma x \rangle$ is obtained from Eq. (2) [or Eq. (4)] by putting x under the integral sign.

For isotropic elastic scattering, Eq. (2) reduces to

$$\langle \sigma \rangle = \frac{p_1}{2} \frac{\gamma_1}{\gamma_1 + 1} \int^{p_F} (1 - 2F + E_2/E_1) P(p_2) dp_2 \times \int_{-1}^1 \frac{A+1}{A} \frac{\sigma d \cos\omega}{(p_1^2 + p_2^2 + 2p_1 p_2 \cos\omega)^{1/2}}, \quad (4)$$

where we have $F = E_F/E_1$ and σ , the total free-particle scattering cross section, is a function of E'' . The lower limit of the first integral sign is zero for $E_1 \geq 2E_F$. For $E_1 < 2E_F$, we have $E_2 = 2E_F - E_1$. In either case the upper limit is p_F , the Fermi momentum. For a Fermi gas, we have

$$P(p_2) dp_2 = 3p_2^2 dp_2 / p_F^3. \quad (5)$$

The solutions of Eqs. (3) and (4) for $E_1 \geq 2E_F$ are given in Tables I-IV. The free-particle cross section is assumed to remain constant with energy in Tables I and II and to vary inversely with energy in Tables III and IV. For nonrelativistic energies we obtain solutions to terms in F^2 (Tables I and III). For relativistic energies F is small. Here we give solutions only to terms in F (Tables II and IV). In these tables σ_0 is the free-particle cross section at the incident energy E_1 when the struck particle is at rest.

We do not give any expressions for the condition $E_1 < 2E_F$, because the impulse approximation implicit

in this entire treatment is not valid at low energies. However, they can be derived from Eq. (4) by setting the lower limit of the first integral equal to $(4E_F - 2E_1)^{1/2}$.^{5,6} In addition to $\langle \sigma \rangle$, for allowed collisions we list $\langle p_2 \rangle$, the average value of the initial momentum, p_2 , of the struck particle; $\langle \cos\omega \rangle$, the average value of the cosine of the collision angle; $\langle p_2 \cos\omega \rangle_{\cos\omega > 0}$ and $\langle p_2 \cos\omega \rangle_{\cos\omega < 0}$, the average value of the projection of p_2 on the beam direction, for positive and negative values of $\cos\omega$, respectively; and $\langle p_2 \sin\omega \rangle$, the average absolute value of the projection of p_2 on the plane perpendicular to the beam direction.

The expression for $\langle \sigma \rangle$ in Eq. (a) of Table I was originally derived by Goldberger.³ The derivation of $\langle \sigma \rangle$ has also been given for the case where σ varies as $1/E''$ or as $1/(E'' + \text{constant})$.

The solutions of Eqs. (3) and (4) given here are for like-particle scattering or for the unlike-particle case where the Fermi energy of the proton is identical to that of the neutron. Equations (2) to (4) can also be solved for different values of the Fermi energy, as in the case of nuclei with unequal numbers of neutrons and protons. We denote E_F/E_1 for the proton by F_p and for the neutron by F_n . Here, we have

$$\langle \sigma \rangle = \frac{1}{2} (\langle \sigma \rangle_{F=F_p} + \langle \sigma \rangle_{F=F_n}), \quad (6)$$

where $\langle \sigma \rangle_{F=F_p}$ and $\langle \sigma \rangle_{F=F_n}$ are the solutions of Eq. (2) or (4). The quantities $\langle x \rangle$ can be obtained in a similar fashion for this case.

In this section we have derived expressions for elastic isotropic scattering. The analytical solution of Eq. (2) for nonisotropic scattering is difficult because of the complexity of the experimental data.¹¹ It is, therefore, not presented here. Furthermore, the expressions given in Tables I to IV will be sufficient for the later discussion.

A machine computation was performed for the solution of the general case.

COMPUTATION

The complex nature of nucleon-nucleon scattering compelled us to evaluate $\langle \sigma \rangle$ and the quantities related to the struck nucleon by means of machine computation (IBM 701) for the actual experimental data. This complexity is especially marked for the higher bombarding energies where both nonisotropic and inelastic scattering are prominent.¹¹

The values of $\langle \sigma \rangle$ for the general case [Eq. (2)] were computed for each value of E_1 by means of the Monte Carlo method from

$$\langle \sigma \rangle = \frac{\sum \epsilon \beta'' d\sigma/d\Omega}{\beta_1 \sum (d\sigma/d\Omega)/\sigma}. \quad (7)$$

where the sums are taken over a sequence of random-number quadruples, related to the kinematical variables by Eqs. (8)-(11). Here we have $\epsilon = 1$, if the energy of

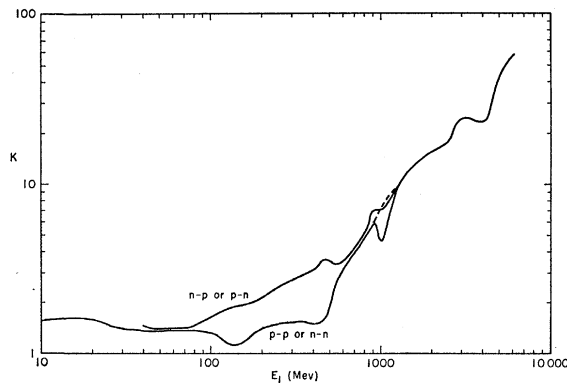


FIG. 1. The variation of K in the expression $\langle \sigma \rangle = \sigma_0(1 - KE_F/E_1)$ for elastic nucleon-nucleon collisions as a function of the energy, E_1 , of the incident nucleon. Like-particle collisions are indicated by $p-p$ or $n-n$, unlike-particle collisions by $n-p$ or $p-n$.

both particles after the collision is greater than E_F , or $\epsilon=0$ otherwise. The quantities β'' and σ depend on p_2 and ω ; $d\sigma/d\Omega$ on p_2 , ω , θ' ; and ϵ on p_2 , ω , θ' , and Φ' [see Eq. (1) and reference 10]. The four independent variables necessary to evaluate each entry in Eq. (7) were obtained from the following relationships:

$$p_2 = \xi_1^{1/2} p_F, \quad (8)$$

$$\cos\omega = 1 - 2\xi_2, \quad (9)$$

$$\cos\theta' = 1 - 2\xi_3, \quad (10)$$

$$\Phi' = 2\pi\xi_4, \quad (11)$$

where each ξ is a random number in the interval 0 to 1, chosen by a method given by Taussky and Todd.¹²

For convenience in machine computation, we have expressed $d\sigma/d\Omega$ in the form of power-series functions of E'' and $\cos\theta'$.¹³ Only nuclear scattering was included. The contribution of Coulomb scattering was subtracted. In this report we consider only those inelastic collisions that lead to pion production. The formation of other particles is neglected. We were not able to correlate all the available data on pion production in a form suitable for machine computation. Instead we derived expressions for the energy of each nucleon resulting from inelastic collisions, based on two different assumptions about the kinetics of the reaction. In the first, the momentum vectors of the pions and nucleons in the center-of-mass system were all assumed to be in the same plane and to be equal in magnitude. The angles between these vectors were taken to be equal. In the second, the momentum of the pions in the center-of-mass system was taken to be zero.

Each successive entry in Eq. (7) was evaluated by means of a new set of values for the four ξ 's. Equations (8)–(11) give the correct distribution of values for each of the variables. After each 100 entries, $\langle\sigma\rangle$ was evaluated for all the cases to that point for the given E_1 . The computation was terminated when the value of $\langle\sigma\rangle$ varied by less than 0.375% for three successive sets of 100 entries. If this test was not satisfied but $\langle\sigma\rangle$ was less than 3.2 mb, the computation was terminated. This exception was made to avoid excessive use of the computer for evaluating $\langle\sigma\rangle$ to a precision not justified by the scattering data. Approximately 1000 to 10 000 entries in Eq. (7) were required for each value of E_1 .

The values of $\langle p_2 \rangle$, $\langle \cos\omega \rangle$, and the other properties of the struck nucleon in allowed collisions were calculated from the relation

$$\langle x \rangle = \frac{\sum x \epsilon \beta'' d\sigma/d\Omega}{\sum \epsilon \beta'' d\sigma/d\Omega}, \quad (12)$$

simultaneously with the other determinations. We did

not compute the final directions of motion of the nucleons and pions (or the energies of the latter), because these would have required an extensive elaboration of the computer program.

RESULTS

In this section we present the results of the machine computation of $\langle\sigma\rangle_{\text{elastic}}$ and $\langle\sigma\rangle_{\text{inelastic}}$ by Eq. (7) and the quantities, $\langle p_2 \rangle$, $\langle \cos\omega \rangle$, etc., by Eq. (12) for collisions between like particles, p - p and n - n , and between unlike particles, p - n and n - p , as a function of the energy of the incident particle. For convenience, we designate the like-particle case by " p - p or n - n " and the unlike-particle case by " n - p or p - n ". We compare these results with the expressions of Tables I–IV.

$\langle\sigma\rangle$ Elastic

The values of $\langle\sigma\rangle$ elastic for different values of E_F were fitted to the equation,

$$1 - \langle\sigma\rangle/\sigma_0 = KE_F/E_1 = KF, \quad (13)$$

by the least-squares method with a deviation of several percent or less. Here K is a constant at each value of E_1 , the incident energy, for $E_F \leq E_1/2$. This type of fit is suggested by Eqs. (a) of Table I and II. The values of K are plotted in Fig. 1. The results shown for $E_1 > 50$ Mev were calculated with $E_F = 18.8$, 24.5, 28.5, and 33.4 Mev. The computed values of $1 - \langle\sigma\rangle/\sigma_0$

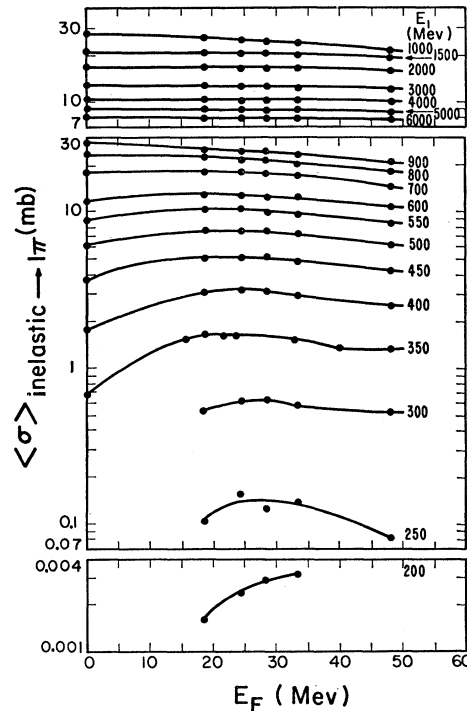


FIG. 2. The values of $\langle\sigma\rangle$ in inelastic nucleon-nucleon collisions for single-pion production based on the assumption that the center-of-mass momenta of the pion and the nucleons are equal.

¹² O. Taussky and J. Todd, in *Symposium on Monte Carlo Methods*, 1954, edited by Herbert A. Meyer (John Wiley & Sons, New York, 1956), p. 18.

¹³ T. P. Clements and L. Winsberg, University of California Radiation Lab. Rept. UCRL-9043 (1960) (unpublished).

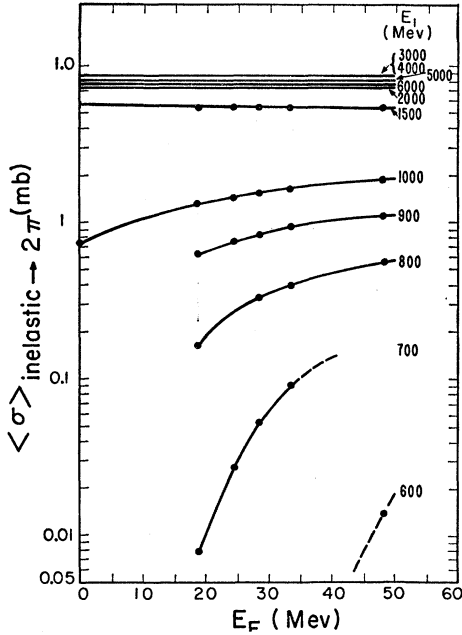


FIG. 3. The values of $\langle \sigma \rangle$ in inelastic nucleon-nucleon collisions for double-pion production based on the assumption that the center-of-mass momenta of the pions and the nucleons are equal.

at $E_F = 48.1$ MeV agree within several percent with Eq. (13) for the values of K given in Fig. 1. The dip in the value of K_{p-p} or $n-n$ at 1 BeV in Fig. 1 is due to a corresponding apparent dip in the free-particle cross section.^{11,13} The dashed line is drawn through the value of K that would result if this anomaly were not present.¹⁰

In general the neutron and proton Fermi energies are different for any given nucleus. Figure 1 is still valid for collisions between like particles. In the case of collisions between unlike particles we have found the following relations to fit the data very well, even if the Fermi energy of one particle is zero:

Neutron Fermi energy is larger than proton Fermi energy, or $F_n > F_p$:

(a) Incident particle is a neutron,

$$1 - \langle \sigma \rangle / \sigma_0 = K_{n-p \text{ or } p-n} (0.7F_n + 0.3F_p). \quad (14)$$

(b) Incident particle is a proton

$$1 - \langle \sigma \rangle / \sigma_0 = K_{n-p \text{ or } p-n} (0.5F_n + 0.5F_p). \quad (15)$$

Corresponding equations can be written for $F_p > F_n$. The values of K_{n-p} or $p-n$ are plotted in Fig. 1. These relations agree closely with Eq. (6).

$\langle \sigma \rangle$ Inelastic

The values of $\langle \sigma \rangle$ for inelastic collisions were evaluated separately for the cases involving the production of one, two and three pions by means of Eq. (7). The values of E_F used here were the same as those given above for the elastic case.

TABLE V. The ratio of $\langle \sigma \rangle_{\text{inelastic}}$ for $p_{\text{c.m.}} = 0$ to $\langle \sigma \rangle_{\text{inelastic}}$ for $p_{\text{c.m.}} = p_{\text{nucleon(c.m.)}}$ for one-, two-, and three-pion production.

One pion ^a		Two or three pions ^c	
E_1 (MeV)	Ratio	E_1 (MeV)	Ratio
400	0.91 ± 0.04^b	900	0.86 ± 0.03^d
700	0.93 ± 0.02	1000	0.89 ± 0.04^d
1000	0.95 ± 0.01	2000	0.96 ± 0.02
≥ 4000	0.99 ± 0	≥ 4000	0.98 ± 0.01

^a Ratio increases with increasing E_F .

^b These values are for $18.8 \text{ MeV} \leq E_F \leq 33.4 \text{ MeV}$. At $E_F = 48.1 \text{ MeV}$, ratio = 1.16.

^c Ratio decreases with increasing E_F .

^d Only for two-pion production, $\sigma(3\pi \text{ production}) = 0$.

The resulting values of $\langle \sigma \rangle$ for like-particle collisions, based on the assumption that the center-of-mass momenta of the pions and nucleons are all equal, are shown in Figs. 2-4. These values are not very different from those based on the other assumption about the pion momentum—that it is zero in the center-of-mass system—as can be seen from Table V. The ratios given in Table V are the same for the like- and the unlike-particle cases at the same value of E_F . Each value given in Table V is the average for the five different Fermi energies. The value following the \pm sign is the average deviation of the individual values from this mean value and results from the variation of the ratio with the Fermi energy. For single-pion production the ratio increases with increasing Fermi energy. For two- and three-pion production the ratio decreases as E_F increases. With this information and the values given in Table V, we can obtain the ratio at each of the five values of E_F . The ratios for other values of E_1 can be obtained by interpolation. The values estimated in this way agree to within 1 or 2% with the values computed directly.

The value of $\langle \sigma \rangle$ for unlike-particle collisions can be obtained by multiplying the values for the like-particle collisions given in Figs. 2-4 by the ratio of the two

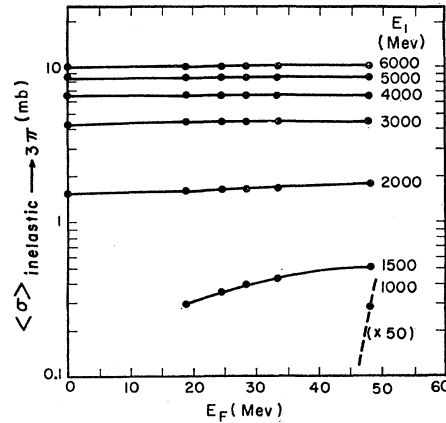


FIG. 4. The values of $\langle \sigma \rangle$ in inelastic nucleon-nucleon collisions for triple-pion production based on the assumption that the center-of-mass momenta of the pions and the nucleons are equal.

TABLE VI. $\langle\sigma\rangle_{n-p}$ or $p-n/\langle\sigma\rangle_{p-p}$ or $n-n$, for inelastic collisions involving one-, two-, and three-pion production.

E_1 (MeV)	One pion	Two or three pions
200	0.44 ± 0.06	
250	0.51 ± 0.02	
300	0.55 ± 0.01	
350 to 700	0.58 ± 0	$0.56 \pm 0.03^{b,c}$
800	0.60 ± 0.01	0.64 ± 0.02^e
900	0.62 ± 0.01	0.69 ± 0.02^e
1000	0.65 ± 0.01	0.75 ± 0.03^e
1500 ^a	0.97 ± 0.01	1.05 ± 0^d
2000 ^a	1.14 ± 0.01	1.17 ± 0^e
3000	1.06 ± 0	1.15 ± 0.01
≥ 4000	1.00 ± 0	1.05 ± 0
		1.00 ± 0

^aRatio decreases with increasing E_F , ratio is constant or increases with increasing E_F for all other cases.

^bDouble-meson production begins at 600 MeV for $E_F \geq 33.4$ MeV. (see Fig. 3).

^cOnly for two-pion production, $\sigma(3\pi \text{ production}) = 0$.

^dFor two-pion production.

^eFor three-pion production.

cross sections, given in Table VI. These values of $\langle\sigma\rangle_{n-p}$ or $p-n/\langle\sigma\rangle_{p-p}$ or $n-n$ are identical for the two assumptions about the pion momentum in the center-of-mass system. The values following the \pm sign are average deviations from the mean and indicate the magnitude of the trend of the ratios with E_F . For $E_1 \leq 1000$ MeV, the ratio increases as E_F increases for all three cases of pion production. At 1500 and 2000 MeV, the variation is in the opposite direction.

$$\langle p_2 \rangle, \langle \cos \omega \rangle, \langle p_2 \cos \omega \rangle_{\cos \omega > 0}, \langle p_2 \cos \omega \rangle_{\cos \omega < 0}, \text{ and } \langle p_2 \sin \omega \rangle$$

The values of $\langle p_2 \rangle$, $\langle \cos \omega \rangle$, $\langle p_2 \cos \omega \rangle_{\cos \omega > 0}$, $\langle p_2 \cos \omega \rangle_{\cos \omega < 0}$, and $\langle p_2 \sin \omega \rangle$ were evaluated by means of Eq. (12) for elastic and inelastic collisions. We consider the elastic case first.

The values of $\langle p_2 \rangle/p_F$ obtained in this manner are plotted in Fig. 5 as a function of E_1 for $E_F = 18.8$ MeV ($0.020m_0c^2$). Similar results are obtained for other values of E_F .¹⁰ The curve shown in Fig. 5 was calculated from Eq. (b) of Tables I-IV. The values of $\langle p_2 \rangle$ calculated for $\sigma = \text{constant}$ and for $\sigma \sim 1/E''$ agree within a fraction of a percent. The values obtained from these equations and from equivalent expressions for $F > \frac{1}{2}$ agree closely with computed values for all the elastic cases investigated, involving both like-particle and unlike-particle collisions.

The computed values of $\langle \cos \omega \rangle$ and those of the average of various projections of the momenta of the struck particle are also shown in Fig. 5. Similar results are obtained for $E_F = 33.4$ MeV.¹⁰ The computed values agree closely with the curves calculated by using the appropriate equations given in Tables I-IV. The agreement is best for $\langle p_2 \rangle$ and for $\langle p_2 \sin \omega \rangle$. Thus, for $E_1 < 200$ MeV the equations in Tables III and IV fit the computed values quite well. Here, the experimentally determined cross sections are isotropic and vary inversely with energy, and the agreement is good. At higher

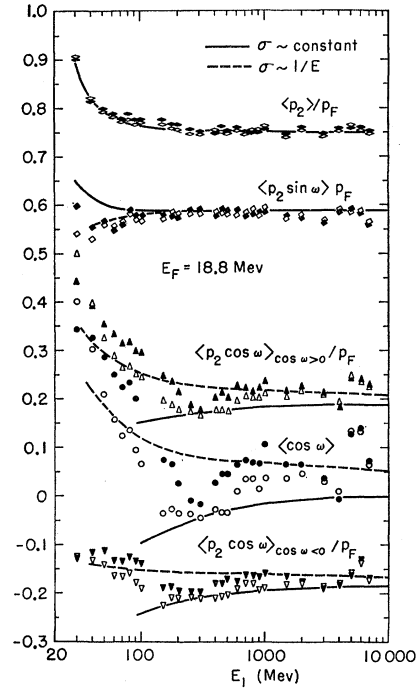


FIG. 5. Average values of quantities related to the struck nucleons in elastic collisions for $E_F = 18.8$ MeV. The momentum of the struck particle is p_2 , the Fermi momentum is p_F , and the collision angle is ω . Computed values are indicated by open symbols for like-nucleon collisions and by closed symbols for collisions between unlike nucleons. Values calculated by using the equations in Tables I-IV are indicated by solid lines for $\sigma = \text{constant}$ and by dashed lines for $\sigma \sim 1/E''$. The solid and dashed lines coincide for $\langle p_2 \rangle/p_F$.

energies the equations in Tables I and II fit the like-particle results better. Here, the cross sections are nearly constant. This is not the case for collisions between unlike particles. For such collisions a clear-cut comparison cannot be made because the angular distributions are not isotropic. Above approximately 500 MeV the like-particle collisions become increasingly nonisotropic. However, at these energies both types of relativistic formulations in Tables II and IV converge to the values that one would expect without the imposition of the exclusion principle. The two formulations appear to be equally good (or bad).

A similar set of comparisons is made in Fig. 6 for the inelastic case for $E_F = 18.8$ MeV. Here too, the equations in Tables II and IV give values that agree with the computed results in the multi-Bev region of bombarding energies. At energies closer to the thresholds for single- and for multiple-pion production, strong deviations occur. The deviations shown in Fig. 6 are to be expected. Large values of p_2 and ω are favored, for these result in the largest center-of-mass energies and hence the largest cross sections. This is due to the sharp rise in the free-particle inelastic cross section with energy above the threshold.¹¹ Similar results are obtained at other values of E_F .¹⁰

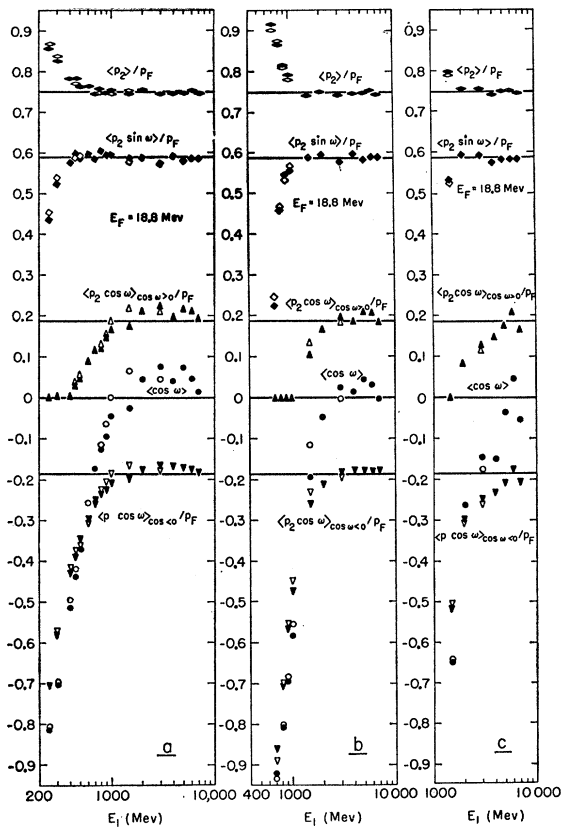


FIG. 6. Average values of quantities related to the struck nucleons in inelastic collisions resulting in the production of 1 (see *a*), 2 (*b*), and 3 (*c*) pions for $E_F = 18.8$ Mev. For notation, see Fig. 5. The values given by the equations in Tables I-IV for $F=0$ are indicated by the horizontal lines. (The value for $\langle \cos \omega \rangle$ is 0 since $p_F=0$ when $F=0$.)

SUMMARY

The effect of the exclusion principle on the elastic cross section is large even at high incident energies, as can be seen from the values of K in Fig. 1. Thus at energies above approximately $\frac{1}{2}$ Bev both the like-particle and unlike-particle effective cross sections are smaller than the free-particle cross sections by about 30% for $E_F \approx 50$ Mev.¹⁰ This is due to the strong forward scattering at these energies, which counterbalances the effect of the decreasing values of E_F/E_i . For incident energies below approximately 100 Mev the computed values of K agree with the values expected from Eq. (a) of Tables I-IV, as do the values

of K_{p-p} or $n-n$ between 200 and 450 Mev (see Fig. 1). The dip in the like-particle curve of Fig. 1 at 150 Mev is due to a change in the way the free-particle cross section varies with energy.¹¹

The values of $\langle \sigma \rangle_{\text{inelastic}}$ show the effects of both the exclusion principle and the rapid rise of the free-particle inelastic cross section near the threshold. The effect of the latter is pronounced at lower energies, resulting in an increase in $\langle \sigma \rangle_{\text{inelastic}}$ as E_F increase (see Figs. 2-4). At intermediate energies, the effect of exclusion causes a small drop in $\langle \sigma \rangle_{\text{inelastic}}$ for single- and double-pion production (Figs. 2 and 3). The effect is more noticeable for single-pion production. At the highest energies the inelastic cross sections are essentially unaffected by the exclusion principle. It is our hope that the values of $\langle \sigma \rangle$ given here will be useful in the interpretation of nuclear cross-section measurements.

The values of $\langle p_2 \rangle$, $\langle \cos \omega \rangle$, and the other quantities in elastic collisions can be determined either by machine computation or from the equations given in Tables I-IV. Agreement between the two methods, while not complete, is probably adequate for many purposes. The values for inelastic collisions near the threshold for pion production deviate strongly from those given by the analytical expressions. This is not surprising since the latter were obtained for elastic collisions. As the bombarding energy increases, the values of these quantities for both elastic and inelastic collisions converge to the original values of these quantities before the collision.

One possible application of these results is in the interpretation of recoil experiments.¹⁴ Some high-energy reactions involve the ejection of a single particle. An example of this type is the (p, pn) reaction, such as $\text{Cu}^{65}(p, pn)\text{Cu}^{64}$. If both the incident and the struck particles leave the nucleus without further interaction, the nucleus left behind (Cu^{64} in the example given here) will recoil with a momentum which depends on that of the ejected nucleon. The momentum of the recoiling nucleus can be measured.¹⁴ Comparisons of this type with the values of $\langle p_2 \rangle$, $\langle p_2 \sin \omega \rangle$, and $\langle p_2 \cos \omega \rangle$ may provide an effective probe of the momentum distribution of the nuclear particles.

ACKNOWLEDGMENT

We wish to thank Professor A. L. Turkevich for his helpful advice.

¹⁴ B. G. Harvey, Ann. Rev. Nuclear Sci. **10**, 235 (1960).